Delay-Coupled Mathieu Equations in Synchrotron Dynamics

Alexander Bernstein[1†], Richard Rand[2]

[1]Center for Applied Mathematics, Cornell University
[2]Dept. of Mathematics and Dept. of Mechanical and Aerospace Engineering, Cornell University

Abstract

This paper investigates the dynamics of two coupled Mathieu equations. The coupling functions involve both delayed and nondelayed terms. We use a perturbation method to obtain a slow flow which is then studied using Routh-Hurwitz stability criterion. Analytic results are shown to compare favorably with numerical integration. The numerical integrator, DDE23, is shown to inadvertently add damping. It is found that the nondelayed coupling parameter plays a significant role in the system dynamics. We note that our interest in this problem comes from an application to the design of nuclear accelerators.

1 Introduction

In this paper we investigate the dynamics of the system of two delay-coupled Mathieu equations:

$$\ddot{x} + \varepsilon\mu\dot{x} + (\delta + \varepsilon\cos t)x = \varepsilon\beta(x(t-T) + y(t-T)), \tag{1}$$

$$\ddot{y} + \varepsilon\mu\dot{y} + (\delta + \varepsilon\cos t)y = \varepsilon\beta(x(t-T) + y(t-T)) + \varepsilon\alpha x. \tag{2}$$

Coupled Mathieu equations without delay have been investigated previously [1], [2]. Recent research has involved systems which combine parametric excitation with delay [3].

Our interest in Eqs.(1) and (2) comes from an application in the design of nuclear accelerators.

1.1 Application

This work was motivated by a novel application in nuclear physics, namely the dynamics of a generic particle accelerator. Since this application is expected to be unfamiliar to most readers of this journal, we offer the following description of a synchrotron [4].

The synchrotron is a particle accelerator in which a "particle" actually consists of a group of electrons in a "bunch." We ignore the interactions of electrons inside each bunch and treat the entire bunch as a single particle.

[†]Corresponding author.
Email address: rrand1@twcny.rr.com

Each bunch leaves an electrical disturbance behind it as it traverses around the synchrotron, and these wake fields are the main source of coupling in the model. The coupling is mediated by several sources, including resistive wall coupling, ion coupling, and the electron cloud effect. The wake fields can persist through entire orbits.

The ensemble of all bunches is called a "train." When a train is modeled as several interacting bunches, each bunch is coupled to the wake of the bunch in front of it. When a train is modeled as a single particle, the train interacts with itself after a full orbit. We will combine both of these into one cohesive model.

Particle paths in the synchrotron are circle-like, but are not exact circles. Since the synchrotron lacks a central force, the circle-like particle orbits are achieved through the use of about 100 electromagnets spread around the periphery. (see Fig. 1).
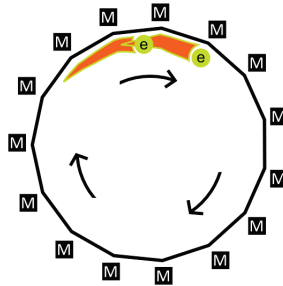

Fig. 1 Two bunches moving clockwise along a polygonal path through the use of a system of electromagnets.

This means that the magnetic external forcing is periodic in rotation angle θ; assuming that the angular velocity of the bunch is constant with $\theta = \omega t$, the forcing is periodic in time as well. We can express this forcing function as a Fourier series, and we shall approximate this series by the first couple of terms in it, namely the constant term and the first cosine term.

We model each bunch as a scalar variable $x_i(t), i = 1, \ldots, n$. Here x_i is the vertical displacement above equilibrium of the center of mass of the ith bunch. Each x_i is modeled as a damped parametrically-forced oscillator, and we write:

$$
\begin{aligned}
\ddot{x}_1 + \varepsilon\mu\dot{x}_1 + (\delta + \varepsilon\cos t)x_1 &= \beta\sum_{j=1}^{n} x_j(t-T) \\
\ddot{x}_i + \varepsilon\mu\dot{x}_i + (\delta + \varepsilon\cos t)x_i &= \beta\sum_{j=1}^{n} x_j(t-T) + \alpha x_{i-1}, \quad i = 2,\ldots,n.
\end{aligned}
\tag{3}
$$

The coupling terms on the right hand side may be modeled as consisting of two types [5]:

    i) plasma interactions,
    ii) resistive wall coupling.

In the case of plasma interactions, the radiation from a bunch produces an electron cloud which travels behind the bunch and influences the dynamics of the next bunch in the train. This results in a coupling term of the form:

$$\alpha x_{i-1}.$$

Resistive wall coupling arises from the finite conductivity of the beam pipe. The skin effect produces a long tail which may be modeled as a delay term, the duration of the delay being the transit time around the ring. The entire train can be modeled as a single superparticle with displacement equal to

the train average, each bunch receiving the same force. This results in a coupling term of the form:

$$\beta \sum_{j=1}^{n} x_j(t-T),$$

where $T =$ delay.

The simplest case is a single bunch, $n = 1$, in which we only consider the effect of delayed self-feedback:

$$\ddot{x} + (\delta + \varepsilon \nu \cos t)x = \beta x(t-T). \tag{4}$$

A system of this type has been investigated by Morrison and Rand [3]. It was shown that the region of instability associated with 2:1 subharmonic resonance can be eliminated by choosing the delay T appropriately.

In this paper we investigate the dynamics of the system (1), (2). The method of two-variable expansion is used to obtain a slow flow whose stability is analyzed. We use the Routh-Hurwitz criteria for calculating stability and compare these results with numerical integration of the system.

2 Two-variable expansion

We start off by transforming the system into a more tractable form. By using the linear transformation:

$$u = x+y, \quad v = x-y, \tag{5}$$

the system (1), (2) becomes

$$\ddot{u} + \varepsilon \mu \dot{u} + (\delta + \varepsilon \cos t)u = \frac{1}{2}\varepsilon \alpha (u+v) + 2\varepsilon \beta u_d, \tag{6}$$

$$\ddot{v} + \varepsilon \mu \dot{v} + (\delta + \varepsilon \cos t)v = -\frac{1}{2}\varepsilon \alpha (u+v), \tag{7}$$

where $u_d \equiv u(t-T)$. These equations have been previously studied in [2] for the special case of $\alpha = 0$, $T = 0$, and $\mu = 0$.

We use the two-variable expansion method [6], [7] to study the dynamics of Eqs. (6), (7). We set

$$\xi(t) = t, \quad \eta(t) = \varepsilon t,$$

where ξ is the time t and η is the slow time.

Since u and v are functions of ξ and η, the derivative with respect to time t is expressed through the chain rule:

$$\dot{u} = u_\xi + \varepsilon u_\eta, \quad \dot{v} = v_\xi + \varepsilon v_\eta.$$

Similarly, for the second derivative we obtain:

$$\ddot{u} = u_{\xi\xi} + 2\varepsilon u_{\xi\eta} + \varepsilon^2 u_{\eta\eta}, \quad \ddot{v} = v_{\xi\xi} + 2\varepsilon v_{\xi\eta} + \varepsilon^2 v_{\eta\eta}.$$

In this paper we only perturb up to $O(\varepsilon)$, and so we will ignore the ε^2 terms.

We then expand u and v in a power series in ε:

$$u(\xi,\eta) = u_0(\xi,\eta) + \varepsilon u_1(\xi,\eta) + O(\varepsilon^2), \quad v(\xi,\eta) = v_0(\xi,\eta) + \varepsilon v_1(\xi,\eta) + O(\varepsilon^2). \tag{8}$$

In addition, we detune off of the 2:1 subharmonic resonance by setting:

$$\delta = \frac{1}{4} + \varepsilon \delta_1 + O(\varepsilon^2). \tag{9}$$

Substituting (8), (9) into (6), (7) and collecting terms in ε, we arrive at the following equations:

$$u_{0,\xi\xi} + \frac{1}{4}u_0 = 0, \tag{10}$$

$$v_{0,\xi\xi} + \frac{1}{4}v_0 = 0, \tag{11}$$

$$u_{1,\xi\xi} + \frac{1}{4}u_1 = -2u_{0,\xi\eta} - \mu u_{0,\xi} - \delta_1 u_0 - u_0 \cos\xi + 2\beta u_{0_d} + \frac{\alpha}{2}(u_0 + v_0), \tag{12}$$

$$v_{1,\xi\xi} + \frac{1}{4}v_1 = -2v_{0,\xi\eta} - \mu v_{0,\xi} - \delta_1 v_0 - v_0 \cos\xi - \frac{\alpha}{2}(u_0 + v_0). \tag{13}$$

The solutions to (10) and (11) are simply:

$$u_0 = A(\eta)\cos(\frac{\xi}{2}) + B(\eta)\sin(\frac{\xi}{2}), \tag{14}$$

$$v_0 = C(\eta)\cos(\frac{\xi}{2}) + D(\eta)\sin(\frac{\xi}{2}). \tag{15}$$

We then substitute (14), (15) into (12), (13). Note that

$$u_{0_d} = A(\eta - \varepsilon T)\cos(\frac{\xi}{2} - \frac{T}{2}) + B(\eta - \varepsilon T)\sin(\frac{\xi}{2} - \frac{T}{2}) \tag{16}$$

Since A and B are unknown functions, the most general way to express them in terms of η is with a Taylor series:

$$A(\eta - \varepsilon T) = A(\eta) - \varepsilon T A' + O(\varepsilon^2) = A(\eta) + O(\varepsilon).$$

Such a technique is common in the literature [3] and is useful for dealing with delay terms.

Trigonometrically expanding equation (16) gives terms in $\cos\frac{\xi}{2}$ and $\sin\frac{\xi}{2}$. The method involves setting the coefficients of such terms equal to zero in order to remove secular terms which cause resonance in equations (12), (13). This results in four equations in four unknowns:

$$A' = -\frac{\alpha D}{2} - 2\beta\mathscr{C}B + \delta_1 B - \frac{\alpha B}{2} - \frac{B}{2} - 2\beta\mathscr{S}A - \frac{\mu A}{2}, \tag{17}$$

$$B' = \frac{\alpha C}{2} - 2\beta\mathscr{S}B - \frac{\mu B}{2} + 2\beta\mathscr{C}A - \delta_1 A + \frac{\alpha A}{2} - \frac{A}{2}, \tag{18}$$

$$C' = \delta_1 D + \frac{\alpha D}{2} - \frac{D}{2} - \frac{\mu C}{2} + \frac{\alpha B}{2}, \tag{19}$$

$$D' = -\frac{\mu D}{2} - \delta_1 C - \frac{\alpha C}{2} - \frac{C}{2} - \frac{\alpha A}{2} = 0, \tag{20}$$

where $\mathscr{S} = \sin(T/2), \mathscr{C} = \cos(T/2)$.

The origin is an equilibrium point of the system; we study its stability, which is determined by the coefficient matrix:

$$\begin{bmatrix} -\frac{4\beta\mathscr{S}+\mu}{2} & -\frac{4\beta\mathscr{C}-2\delta_1+\alpha+1}{2} & 0 & -\frac{\alpha}{2} \\ \frac{4\beta\mathscr{C}-2\delta_1+\alpha-1}{2} & -\frac{4\beta\mathscr{S}+\mu}{2} & \frac{\alpha}{2} & 0 \\ 0 & \frac{\alpha}{2} & -\frac{\mu}{2} & \frac{2\delta_1+\alpha-1}{2} \\ -\frac{\alpha}{2} & 0 & -\frac{2\delta_1+\alpha+1}{2} & -\frac{\mu}{2} \end{bmatrix}. \tag{21}$$

The characteristic polynomial of this matrix is given by:

$$\lambda^4 + p\lambda^3 + q\lambda^2 + r\lambda + s = 0, \tag{22}$$

where

$$p = 4\beta\mathscr{S} + 2\mu, \tag{23}$$

$$q = 4\beta^2\mathscr{S}^2 + 6\beta\mu\mathscr{S} + 4\beta^2\mathscr{C}^2 - 4\beta\delta_1\mathscr{C} + 2\alpha\beta\mathscr{C} + \frac{3\mu^2}{2} + 2\delta_1^2 - \frac{1}{2}, \tag{24}$$

$$r = 4\beta^2\mu\mathscr{S}^2 + 3\beta\mu^2\mathscr{S} + 4\beta\delta_1^2\mathscr{S} + 4\alpha\beta\delta_1\mathscr{S} - \beta\mathscr{S} \tag{25}$$

$$+ 4\beta^2\mu\mathscr{C}^2 - 4\beta\delta_1\mu\mathscr{C} + 2\alpha\beta\mu\mathscr{C} + \frac{\mu^3}{2} + 2\delta_1^2\mu - \frac{\mu}{2},$$

$$s = \beta^2\mu^2\mathscr{S}^2 + 4\beta^2\delta_1^2\mathscr{S}^2 + 4\alpha\beta^2\delta_1\mathscr{S}^2 + \alpha^2\beta^2\mathscr{S}^2 - \beta^2\mathscr{S}^2 \tag{26}$$

$$+ \frac{\beta\mu^3\mathscr{S}}{2} + 2\beta\delta_1^2\mu\mathscr{S} + 2\alpha\beta\delta_1\mu\mathscr{S} - \frac{\beta\mu\mathscr{S}}{2} + \beta^2\mu^2\mathscr{C}^2$$

$$+ 4\beta^2\delta_1^2\mathscr{C}^2 + 4\alpha\beta^2\delta_1\mathscr{C}^2 + \alpha^2\beta^2\mathscr{C}^2 - \beta^2\mathscr{C}^2 - \beta\delta_1\mu^2\mathscr{C}$$

$$+ \frac{\alpha\beta\mu^2\mathscr{C}}{2} - 4\beta\delta_1^3\mathscr{C} - 2\alpha\beta\delta_1^2\mathscr{C} + \beta\delta_1\mathscr{C} - \frac{\alpha\beta\mathscr{C}}{2} + \frac{\mu^4}{16}$$

$$+ \frac{\delta_1^2\mu^2}{2} - \frac{\mu^2}{8} + \delta_1^4 - \frac{\delta_1^2}{2} + \frac{1}{16}.$$

We will use the Routh-Hurwitz Criterion on the polynomial (22) to determine the stability of the equilibrium point at the origin.

3 Routh-Hurwitz criterion

In this work, by "linearly stable" we mean bounded in time, not to be confused with asymptotic stability which requires that the motion approaches the equilibrium point as $t \to \infty$. So e.g. if a system has a pair of complex roots with negative real parts and a second pair of purely imaginary roots, we will say that this system is linearly stable.

The Routh-Hurwitz stability criterion [8] is a test on the coefficients of a characteristic polynomial to determine whether the system is linearly stable.

In Routh's original paper [8], he gives an example of a biquadratic polynomial that has the same form as (22). The conditions of stability are given by:

$$p > 0, \quad q > 0, \quad r > 0, \quad s > 0, \quad pqr - r^2 - p^2s \geq 0.$$

To obtain stability plots, we plot the curves $p = 0$, $q = 0$, $r = 0$, $s = 0$, and $pqr - r^2 - p^2s = 0$, which partitions the $T - \delta_1$ plane into disjoint regions. Then we numerically evaluate the quantities p, q, r, and s at representative points in each region. Note that the resulting plots are 4π-periodic in T since the quantities p, q, r and s are 4π-periodic in T.

The first set of parameters we examined was $\mu = 0, \alpha = 0, \beta = 0.125$ (see Fig. 2).

In the case when $\alpha = 0$ and $\mu = 0$, we see that the transformation (5) uncouples the system (1), (2) into a standard Mathieu equation (7) and a delayed Mathieu equation (6); the latter has been studied in [3]. For the system (1), (2) to be stable, both of equations (6), (7) must be stable. Since Eq. (7) with $\alpha = 0$ does not involve delay, it causes instability in the region $|\delta - \frac{1}{4}| < \frac{\varepsilon}{2} + O(\varepsilon^2)$, or from Eq. (9), in the horizontal strip $-0.5 < \delta_1 < 0.5$. See Fig. 2, which agrees with these considerations and the results found in [3].

The next set of parameters we examined was $\mu = 0, \alpha = 0.01, \beta = 0.125$ (see Fig. 3).

It turns out that, for any non-zero value of α (and $\mu = 0$), the Routh-Hurwitz criterion predicts instability almost everywhere! How is it possible that an arbitrarily small value of α can cause a discontinuous change in the stability diagram, from Fig. 2 to Fig. 3? The reason is that in the stable
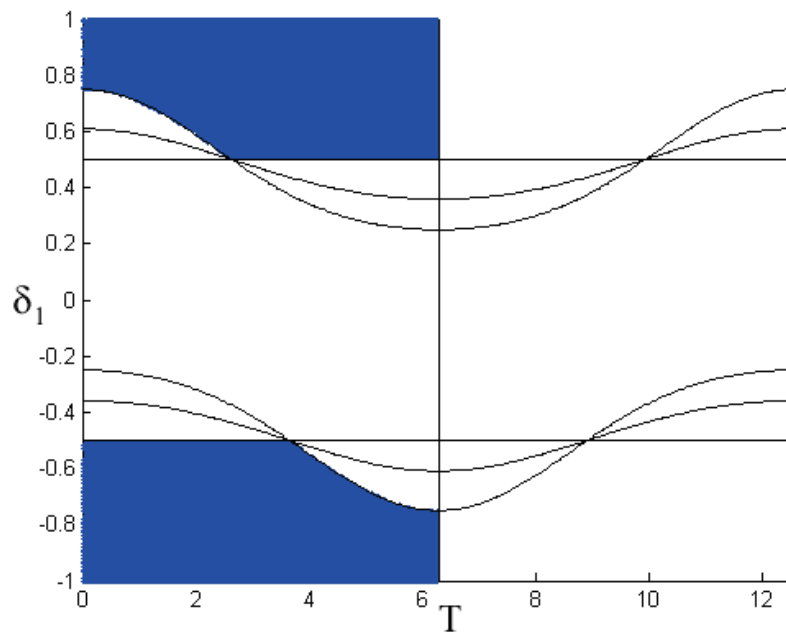
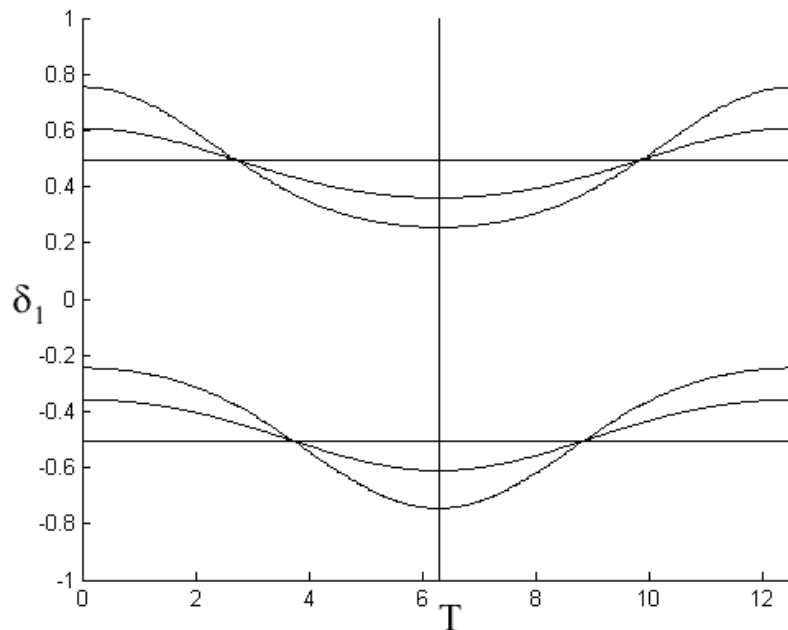$$\mu = 0, \quad \alpha = 0, \quad \beta = 0.125$$

Fig. 2 The shaded regions are stable and the unshaded regions are unstable. The curved lines represent potential stability transition curves for the 5 inequalities in the Routh-Hurwitz criterion. Note that the entire plot is 4π-periodic in T.

$$\mu = 0, \quad \alpha = 0.01, \quad \beta = 0.125$$

Fig. 3 The shaded regions are stable and the unshaded regions are unstable. The curved lines represent potential stability transition curves for the 5 inequalities in the Routh-Hurwitz criterion. Note that the entire plot is 4π-periodic in T.

region of Fig. 2 there are purely imaginary eigenvalues λ, and an arbitrarily small value of α can move these eigenvalues to the right half plane.

The proof of this phenomenon can be seen by examining the $pqr - r^2 - p^2 s \geq 0$ stability condition when $\mu = 0$ (see Eqs. (23)-(26)):

$$\text{For instability } pqr - r^2 - p^2 s = -16\alpha^2\beta^2\mathscr{S}^2(\beta^2 - 2\beta\delta_1\mathscr{C} + \delta_1^2) < 0$$

Note that α^2, β^2, and $\mathscr{S}^2$ are all positive, and so $\beta^2 - 2\beta\delta_1\mathscr{C} + \delta_1^2$ needs to be positive for the system to be unstable.

First note that if $\mathscr{C} = 0$ (i.e. if $\cos\frac{T}{2} = 0$, i.e. if $T = n\pi$, $n = 1, 3, 5, \cdots$) then $\beta^2 - 2\beta\delta_1\mathscr{C} + \delta_1^2$ is positive. Therefore, by continuity, in order for $\beta^2 - 2\beta\delta_1\mathscr{C} + \delta_1^2$ to become negative it must first pass through zero. But the equation

$$\beta^2 - 2\beta\delta_1\mathscr{C} + \delta_1^2 = 0$$

which is a quadratic on δ_1, cannot have real roots δ_1 since the discriminant is

$$4\beta^2(\mathscr{C}^2 - 1) < 0 \text{ if } \mathscr{C}^2 \neq 1$$

Thus for a nonzero value of α (and $\mu = 0$) the system is unstable almost everywhere.

The special case $T = n\pi$, $n = 2, 4, 6, \ldots$, gives $\mathscr{C} = \cos\frac{T}{2} = \pm 1$, and is excluded from this argument; this case may (and indeed does) correspond to a stable region of measure zero in the $T - \delta_1$ plane.

The next set of parameters we examined was $\mu = 0.01, \alpha = 0.01, \beta = 0.125$ (see Fig. 4).

Fig. 4 shows the effect of including nonzero damping to the system of Fig. 3. We find that the stable regions from Fig. 3 return. The introduction of μ also creates much more intricate potential transition curves, although as both α and μ are relatively small, the stable regions remain very similar to those in Fig. 3.

Note that the stability boundary at $T = 4\pi$ has moved slightly to the left.

The next set of parameters we examined was $\mu = 0.1, \alpha = 0.01, \beta = 0.125$ (see Fig. 5).

Here we can see that the effect of increasing μ is to increase the size of the stable region near $T = 2\pi$ and $T = 4\pi$. In particular, the stability boundary near $T = 4\pi$ that appeared in Fig. 5 has moved further to the left, and the edge of the stable region around $T = 2\pi$ has moved to the right. These results reflect our intuition that adding damping increases the stability of the system.

The next set of parameters we examined was $\mu = 0.01, \alpha = 0.1, \beta = 0.125$ (see Fig. 6).

By comparing Fig. 4 with Fig. 6 we see that the effect of increasing α is to decrease the size of the stable region. The remaining stable regions cluster around $T = 0$ and $T = 2\pi$, suggesting that $T = n\pi$, $n = 0, 2, 4, \ldots$ produces stable regions that resist the destabilizing effect of the coupling term α.

We proceed to compare these results to numerical integration.

4 Numerical results

The numerical computations use DDE23 in MATLAB [9] to numerically integrate the original DDE's (1), (2).

These numerical results will be compared to the analytical results presented earlier in the paper. We note that the analytical results are approximate due to a) the perturbation method, which truncates the solution, neglecting terms of $O(\varepsilon^2)$, and b) the replacement of delay terms in the slow flow (17)–(20) by nondelayed terms, a step which is valid for small ε. In this way both the numerical and the analytic approaches are approximate.

Determining the stability of this system via numerical integration is a challenge in and of itself. Specifically, in the limit as $\mu \to 0$, the system becomes Hamiltonian and there is no damping; in this

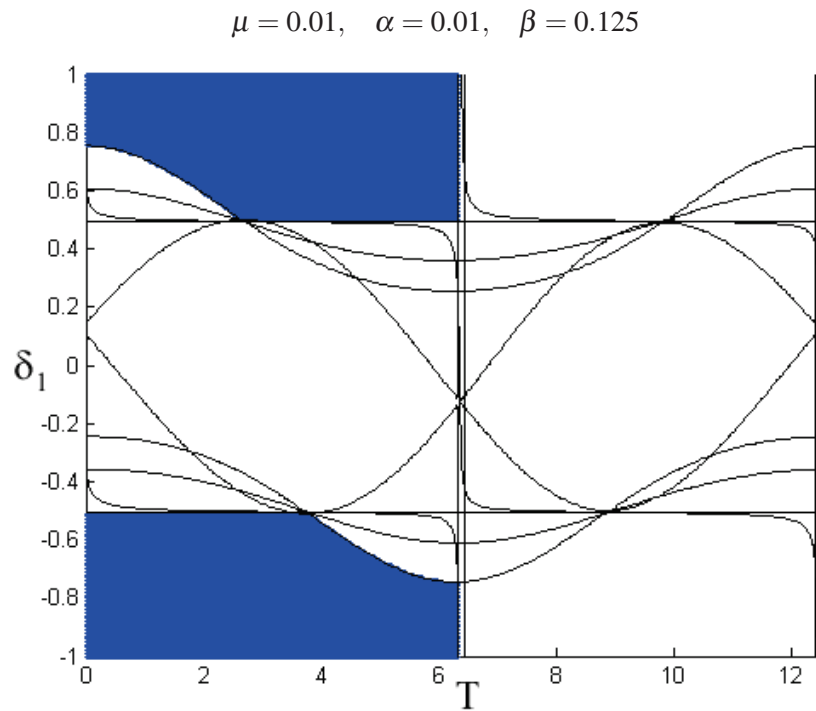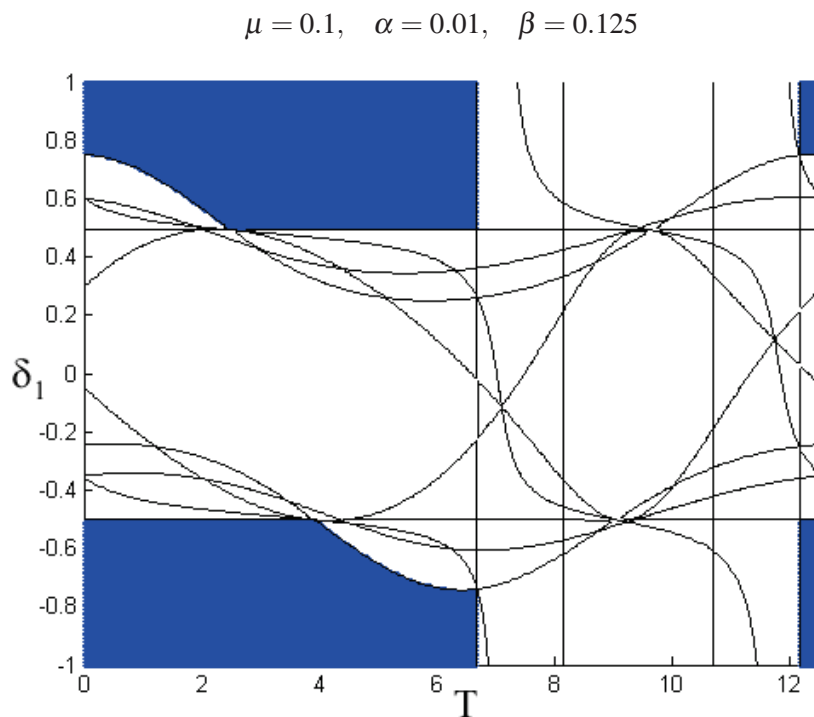$$\mu = 0.01, \quad \alpha = 0.01, \quad \beta = 0.125$$

Fig. 4 The shaded regions are stable and the unshaded regions are unstable. The curved lines represent potential stability transition curves for the 5 inequalities in the Routh-Hurwitz criterion. Note that the entire plot is 4π-periodic in T.

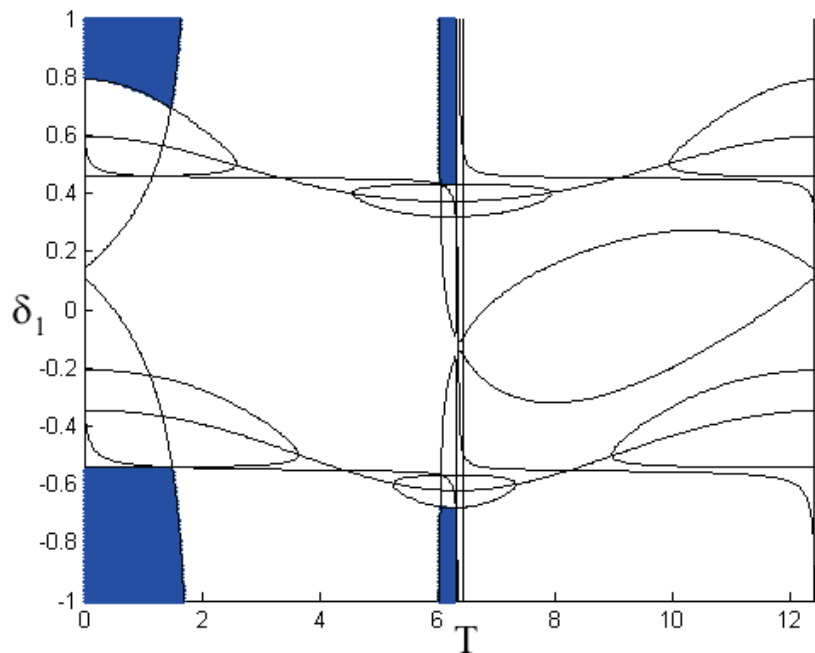$$\mu = 0.1, \quad \alpha = 0.01, \quad \beta = 0.125$$

Fig. 5 The shaded regions are stable and the unshaded regions are unstable. The curved lines represent potential stability transition curves for the 5 inequalities in the Routh-Hurwitz criterion. Note that the entire plot is 4π-periodic in T.

$$\mu = 0.01, \quad \alpha = 0.1, \quad \beta = 0.125$$

Fig. 6 The shaded regions are stable and the unshaded regions are unstable. The curved lines represent potential stability transition curves for the 5 inequalities in the Routh-Hurwitz criterion. Note that the entire plot is 4π-periodic in T.

case a stable solution is one that oscillates, rather than one that approaches a fixed point. Even when damping is present, the general effect of adding delay to the system is to increase the instability.

One of the ways to examine the growth of the system is by calculating the amplitude of the system as a function of time. In this work we measured the amplitude of the motion by computing $\sqrt{x(t)^2 + \dot{x}(t)^2 + y(t)^2 + \dot{y}(t)^2}$. In a stable system, the amplitude will either decrease or oscillate around a finite value. In an unstable system, the amplitude will increase without bound. Thus, a basic test for instability is to integrate over a long time period and compare the amplitude at the final time with the amplitude at an earlier time. In particular we compared the amplitude at time 6000 with the amplitude at time 5000. In all computations we used $\varepsilon = 0.01$.

In Fig. 7 we see that for $\alpha = 0$ and $\mu = 0$ the numerical results closely match the perturbation results. The numerical results for $\alpha = 0.01, \mu = 0.01$ and $\alpha = 0.01, \mu = 0.1$ are also quite similar to their corresponding results from the Routh-Hurwitz criterion (Fig. 4 and Fig. 5).

In Fig. 8 we see that in the case when α is nonzero and μ is zero the numerical results differ quite strongly from the results predicted by the Routh-Hurwitz criterion. Recall from Fig. 3 that the introduction of small α caused instability almost everywhere due to the occurrence of purely imaginary roots in the $\alpha = 0$, $\mu = 0$ case. We believe the failure of the numerical solution to match the analytic solution in Fig. 8 is because the numerical solver is inadvertently adding a small bit of damping to the system due to numerical error.

To estimate the quantity of inherent damping in the numerical solution, we inserted negative values for the damping coefficient μ and adjusted the size of μ so that analytic and numerical results agree. For example, in the case of Fig. 8, we set $\mu = -0.2$ in the numerical results, producing agreement between numerical and analytic results as can be seen in Fig. 9.

In Fig. 10 we see that when α is greater than μ the numerical results and perturbation results do not match. However, in Fig. 11 we see that for an adjusted μ value of $\mu = -0.0375$ the numerical
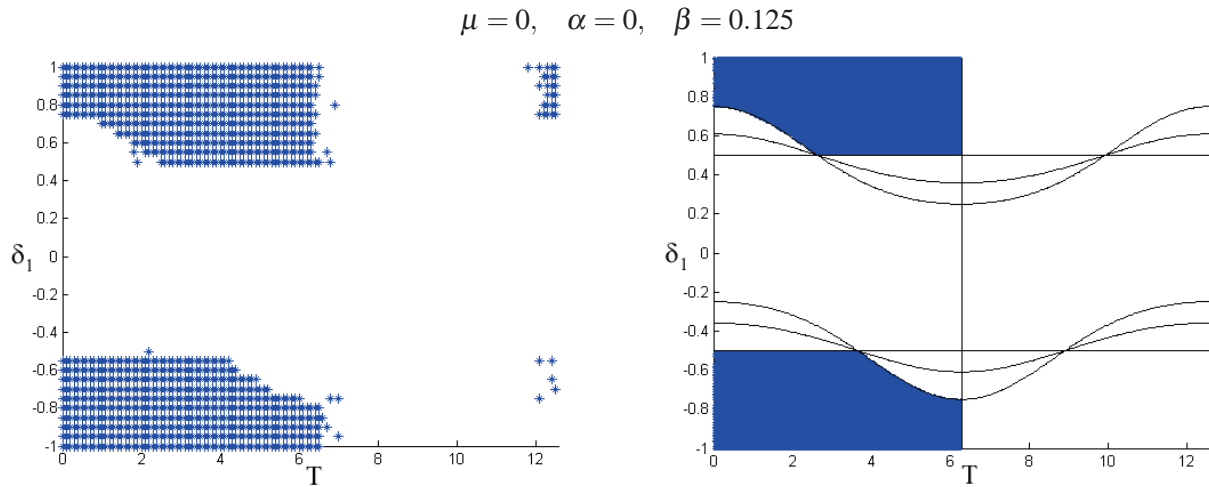
$$\mu = 0, \quad \alpha = 0, \quad \beta = 0.125$$

Fig. 7 The left graph is the result of the numerical integration. The right graph is Fig. 2.

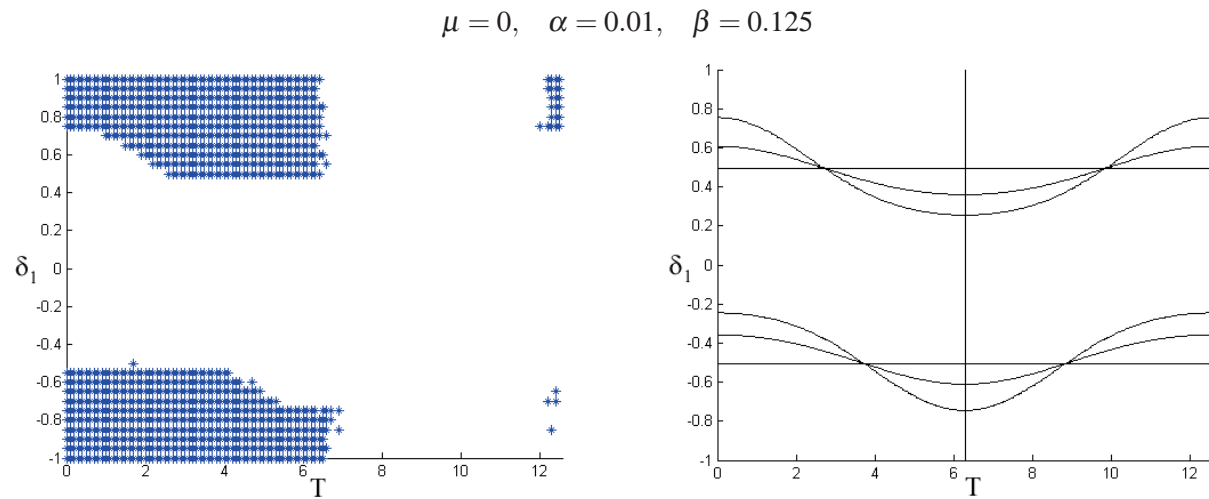$$\mu = 0, \quad \alpha = 0.01, \quad \beta = 0.125$$

Fig. 8 The left graph is the result of the numerical integration. The right graph is Fig. 3.

results more closely match the Routh-Hurwitz results. This outcome is important as it highlights that the inherent damping of the numerical integrator depends on α.

Note that adjusted numerical results show several scattered stable points in regions that are predicted to be unstable. This is not an artifact of the μ adjustment but rather is due to the inaccuracy of the numerical method. The results become more accurate as the numerical integrator runs for longer times. In particular, for Figs. 10, 11 we compared the amplitude at time 8000 with the amplitude at time 6000.

5 Conclusion

In this paper, we investigated the dynamics of two coupled Mathieu equations with delay. In particular we analyzed the stability of the origin and the effect of delay and damping on stability. We used the method of two variable expansion to calculate a characteristic polynomial of the system's slow flow, and used the Routh-Hurwitz criterion to determine stability; these results were then compared with
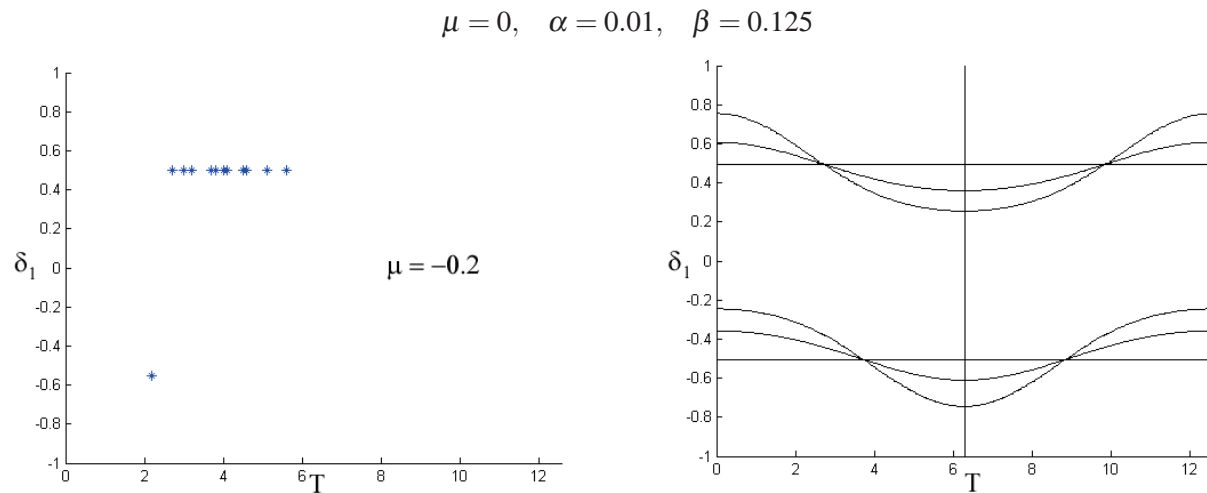
$$\mu = 0, \quad \alpha = 0.01, \quad \beta = 0.125$$

Fig. 9 The left graph is the result of the numerical integration with an adjusted μ value of $\mu = -0.2$. The right graph is Fig. 3.

$$\mu = 0.01, \quad \alpha = 0.1, \quad \beta = 0.125$$
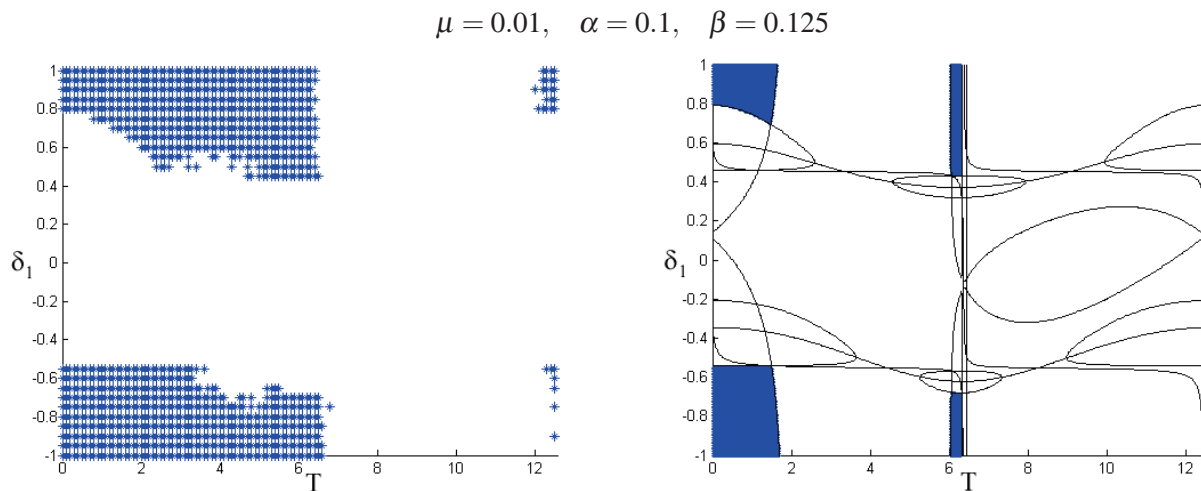

Fig. 10 The left graph is the result of the numerical integration. The right graph is Fig. 6.

numerical integration.

The numerical results closely matched the Routh-Hurwitz criterion when both $\alpha = 0$ and $\mu = 0$, but introducing nonzero values of either of these parameters caused the two methods to yield very different results. We believe this is because the numerical solver implicitly carries its own damping effect. By comparing perturbation results with those of numerical integration we were able to estimate the extent of inherent damping in the numerical integrator DDE23 in MATLAB.

In the parameter range which we explored, we found that increases in α and delay T tended to decrease stability, whereas an increase in damping μ tended to raise stability.

6 Acknowledgments

$$\mu = 0.01, \quad \alpha = 0.1, \quad \beta = 0.125$$
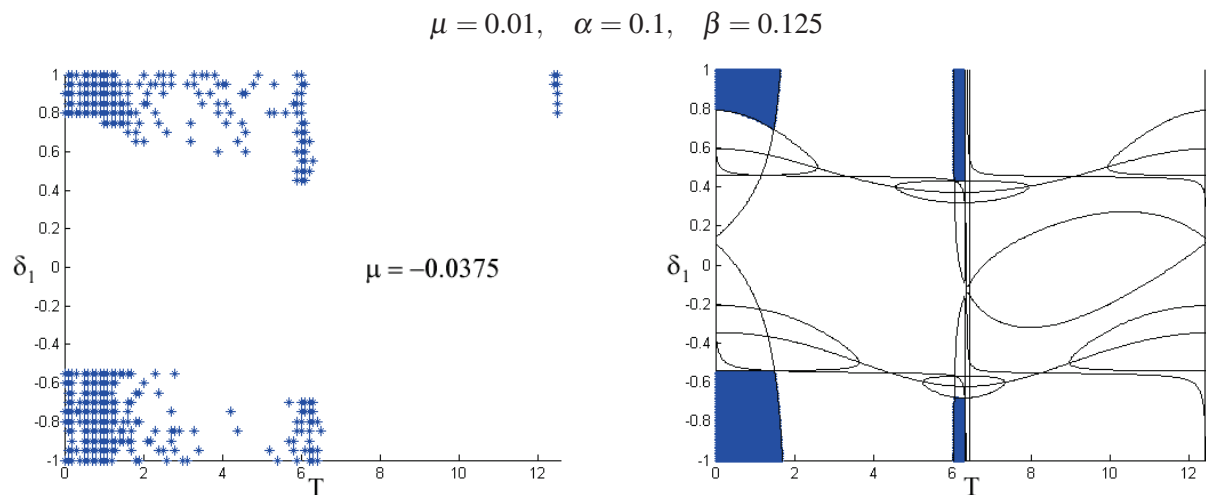

$\mu = -0.0375$

Fig. 11 The left graph is the result of the numerical integration with an adjusted μ value of $\mu = -0.0375$. The right graph is Fig. 6.

References

[1] Hsu, C.S. (1961), On a restricted class of coupled Hill's equations and some applications, *Journal of Applied Mechanics*, **28** (4), Series E, 551.

[2] Bernstein, A. and Rand, R.H. (2016), Coupled Parametrically Driven Modes in Synchrotron Dynamics. Chapter 8, pp.107–112 in *Nonlinear Dynamics, Volume 1: Proceedings of the 33rd IMAC, A Conference and Exposition on Structural Dynamics*, G. Kerschen, editor, Springer.

[3] Morrison, T.M. and Rand, R.H. (2007), 2:1 Resonance in the delayed nonlinear Mathieu equation, *Nonlinear Dynamics*, 341–352. doi:10.1007/s11071-006-9162-5

[4] "Cornell Electron Storage Ring." (2014), *CLASSE: CESR.* 2014 Cornell Laboratory for Accelerator-based Sciences and Education
<http://www.lepp.cornell.edu/Research/CESR/WebHome.html>

[5] Meller, R.E., personal communication to author RR on 12-27-13

[6] Kevorkian, J. and Cole, J.D. (1981), Perturbation Methods in Applied Mathematics, *Applied Mathematical Sciences*, Vol. **34**, Springer.

[7] Rand, R.H. (2012), Lecture Notes in Nonlinear Vibrations, Published on-line by The Internet-First University Press.
<http://ecommons.library.cornell.edu/handle/1813/28989>

[8] Routh, E.J.(1877), *A treatise on the stability of a given state of motion, particularly steady motion*, Macmillan, London, U.K.

[9] MATLAB's reference on dde23. http://www.mathworks.com/help/matlab/ref/dde23.html